ORIGINAL RESEARCH ARTICLE

Detection of precancerous lesions in cervical images of perimenopausal women using U-net deep learning

DOI: 10.29063/ajrh2025/v29i4.10

Na Zhao[1],Yan Gao[2], Fang Li[3], Jingtian Shi[4], Yanni Huang[1] and Hongyun Ma[5]

Department of Gynecology, Peking University First Hospital Ningxia Women and Children's Hospital (Ningxia Hui Autonomous Region Maternal and Child Health Hospital), Yinchuan 750001, Ningxia Hui Autonomous Region, China[1]; Department of Obstetrics and Gynecology, Yinchuan Second People's Hospital, Yinchuan, 750011, Ningxia Hui Autonomous Region, China[2]; Department of Pathology, Peking University First Hospital Ningxia Women and Children's Hospital (Ningxia Hui Autonomous Region Maternal and Child Health Hospital), Yinchuan 750001, Ningxia Hui Autonomous Region, China[3]; Department of Pharmacy, Peking University First Hospital Ningxia Women and Children's Hospital (Ningxia Hui Autonomous Region Maternal and Child Health Hospital), Yinchuan 750001, Ningxia Hui Autonomous Region, China[4]; Department of Obstetrics and Gynecology, People's Hospital of Ningxia Hui Autonomous Region, Ningxia Medical University, Yinchuan 750000, Ningxia Hui Autonomous Region, China[5]

***For Correspondence:** Email: *remarna_525@163.com*

Abstract

Due to physiological changes during the perimenopausal period, the morphology of cervical cells undergoes certain alterations. Accurate cell image segmentation and lesion identification are of great significance for the early detection of precancerous lesions. Traditional detection methods may have certain limitations, thereby creating an urgent need for the development of more effective models. This study aimed to develop a highly efficient and accurate cervical cell image segmentation and recognition model to enhance the detection of precancerous lesions in perimenopausal women. based on U-shaped Network(U-Net) and Residual Network (ResNet). The model integrates U-Net with Segmentation Network (SegNet) and incorporates the Squeeze-and-Excitation (SE) attention mechanism to create the 2Se/U-Net segmentation model. Additionally, ResNet is optimized with the local discriminant loss function (LD-loss) and deep residual learning (DRL) blocks to develop the LD/ResNet lesion recognition model. The performance of the models is evaluated using data from 103 cytology images of perimenopausal women, focusing on segmentation metrics like mean pixel accuracy (MPA) and mean intersection over union (mIoU), as well as lesion detection metrics such as accuracy (Acc), precision (Pre), recall (Re), and F1-score (F1). Results show that the 2Se/U-Net model achieves an MPA of 92.63% and mIoU of 96.93%, outperforming U-Net by 12.48% and 9.47%, respectively. The LD/ResNet model demonstrates over 97.09% accuracy in recognizing cervical cells and achieves high detection performance for precancerous lesions, with Acc, Pre, and Re at 98.95%, 99.36%, and 98.89%, respectively. The model shows great potential for enhancing cervical cancer screening in clinical settings. *(Afr J Reprod Health 2025; 29 [4]: 108-119)*

Keywords: U-Net; ResNet; cervical cell images; perimenopause; precancerous lesion detection

Résumé

En raison des changements physiologiques survenus pendant la période périménopausique, la morphologie des cellules cervicales subit certaines altérations. Une segmentation précise des images cellulaires et une identification des lésions revêtent une grande importance pour la détection précoce des lésions précancéreuses. Les méthodes de détection traditionnelles peuvent présenter certaines limites, créant ainsi un besoin urgent de développement de modèles plus efficaces. Cette étude visait à développer un modèle de segmentation et de reconnaissance d'images de cellules cervicales très efficace et précis pour améliorer la détection des lésions précancéreuses chez les femmes en périménopause. basé sur un réseau en forme de U (U-Net) et un réseau résiduel (ResNet). Le modèle intègre U-Net avec Segmentation Network (SegNet) et intègre le mécanisme d'attention Squeeze-and-Excitation (SE) pour créer le modèle de segmentation 2Se/U-Net. De plus, ResNet est optimisé avec la fonction de perte discriminante locale (LD-loss) et les blocs d'apprentissage résiduel profond (DRL) pour développer le modèle de reconnaissance des lésions LD/ResNet. Les performances des modèles sont évaluées à l'aide des données de 103 images cytologiques de femmes en périménopause, en se concentrant sur les mesures de segmentation telles que la précision moyenne des pixels (MPA) et l'intersection moyenne sur l'union (mIoU), ainsi que les mesures de détection des lésions telles que l'exactitude (Acc), la précision (Pre), le rappel (Re) et le score F1 (F1). Les résultats montrent que le modèle 2Se/U-Net atteint un MPA de 92,63 % et un mIoU de 96,93 %, surpassant U-Net de 12,48 % et 9,47 %, respectivement. Le modèle LD/ResNet démontre une précision de plus de 97,09 % dans la reconnaissance des cellules cervicales et atteint des performances de détection élevées pour les lésions précancéreuses, avec Acc, Pre et Re à 98,95 %, 99,36 % et 98,89 %, respectivement. Le modèle montre un grand potentiel pour améliorer le dépistage du cancer du col de l'utérus en milieu clinique. *(Afr J Reprod Health 2025; 29 [4]: 108-119).*

Mots-clés: U-Net ; ResNet ; images de cellules cervicales ; périménopause ; détection de lésions précancéreuses

Introduction

Perimenopause is a critical phase in a woman's life cycle, typically occurring between the ages of 45 and 55[1]. During this period, women experience great hormonal fluctuations and potential changes in overall health[2]. Precancerous cervical lesions are a significant health risk for women during this time, and their early detection and intervention are crucial for preventing the development of cervical cancer[3]. Currently, cervical image recognition in clinical practice primarily relies on microscopic examination and liquid-based cytology[4]. In recent years, advancements in medical imaging technology and computer-aided diagnostics have made deep learning-based image analysis methods an important research direction in the field of precancerous lesion detection.

U-Net is a widely applied deep learning network architecture originally designed for biomedical image segmentation. Its design is inspired by fully convolutional networks (FCNs) and effectively combines encoding-decoding structures to accurately extract useful features from complex medical images. U-Net features an encoding-decoding architecture with skip connections, providing high precision and accuracy in image segmentation[5]. The successful adoption of U-Net is attributed to its excellent extraction capabilities and retention of image details[6]. In the analysis of cervical images from perimenopausal women, traditional visual inspection and pathological diagnosis methods face challenges in Accuracy and efficiency. The convolutional neural network U-Net combined with an improved level set method is used to segment overlapping cervical smear cells. This model performs well in segmenting individual cells, particularly in regions of cell overlap[7]. Some researchers developed an RGB and Hyperspectral dual-modal pathological image Cross-attention U-Net (CrossU-Net) model based on the U-Net network for the detection of precancerous gastric lesions[8]. The results showed that this model achieved a segmentation accuracy and Dice coefficient of 96.53% and 91.62%, respectively[9]. By incorporating the U-Net deep learning network for automated cancer recognition, not only can the accuracy of detection be improved, but diagnostic efficiency can also be significantly enhanced.

This study aimed to develop an automated precancerous lesion detection system for cervical cancer under the U-Net deep learning model. By analyzing cervical images from perimenopausal women, this study aimed to determine the effectiveness of U-Net in diagnosing precancerous lesions in perimenopausal women, thus providing clinicians with an efficient and reliable auxiliary diagnostic tool. This approach will not only enhance the health outcomes for perimenopausal women but also offer new technological methods for the early prevention and intervention of cervical cancer.

Methods

Experimental data

A total of 103 perimenopausal women admitted to Peking University First Hospital Ningxia Women and Children's Hospital between June 2023 and June 2024 were recruited as the study participants. Peking University First Hospital Ningxia Women and Children's Hospital (Ningxia Hui Autonomous Region Maternal and Child Health Hospital) is a comprehensive hospital integrating medical care, teaching, research, prevention, and healthcare. It has rich clinical experience and a professional medical team in the field of obstetrics and gynecology, as well as advanced medical equipment and technology. All included subjects underwent cervical colposcopy and histopathological examination, with complete cervical cell images available. The patients' ages ranged from 40 to 51 years, with a mean age of 43.36 ± 2.09 years. The inclusion criteria were: i) examination conducted during non-pregnant and non-menstrual periods; ii) maintaining normal sexual activity; iii) avoidance of sexual activity 2-3 days prior to the examination; iv) no vaginal douching or use of vaginal medications before the examination; v) voluntary acceptance of cervical colposcopy and liquid-based cytology; vi) presence of related clinical symptoms such as increased vaginal discharge or cervical contact bleeding.

The exclusion criteria were: i) patients with severe systemic diseases (*e.g.*, cardiac, hepatic, renal

diseases) during the perimenopausal period; ii) patients with a history of malignant tumors; iii) patients who had undergone total hysterectomy, pelvic radiation therapy, or cervical conization; iv) patients unwilling to undergo cervical colposcopy and histopathological examination.

Histopathological examination methods

Samples were collected from subjects in the lithotomy position utilizing a standardized sampler to brush exfoliated cells from the cervix and vaginal surface. The sampler was then placed in cell preservation solution for thorough washing. The samples were centrifuged at 3200 rpm, 16°C for 15 minutes, and the supernatant was discarded. Liquid-based smears were prepared employing the fully automated liquid-based cytology sedimentation staining system produced by Guangzhou Anbiping Pharmaceutical Technology Co., Ltd., and standard Papanicolaou staining was performed. All prepared liquid-based smears were scanned using the Pannoramic MIDI digital pathology slide scanner from 3DHISTECH, Hungary. This scanner features image resolutions of 0.23 μm/pixel (20× objective) and 0.12 μm/pixel (40× objective), converting the smears into high-resolution digital images.

Establishment of cervical cell image segmentation model based on U-Net

Despite improvements made to U-Net based on fully convolutional neural networks, which enhance its robustness and adaptability to small sample datasets, the model structure still has limitations. When using U-Net for cervical cell image segmentation, the model exhibits varying degrees of classification errors across different components of the cervical cells, and extensive misidentifications in some images. U-Net fails to fully restore the relative pixel positions lost during the feature extraction process, leading to issues such as under-segmentation, over-segmentation, and rough edges in cervical cell components[10,11].

SegNet transmits the maximum pooling index information from the pooling layers to the decoder, allowing the restoration of the image's spatial resolution during the decoding process. This approach effectively preserves spatial information in the image, aiding in precise boundary recovery[12]. The decoder portion of SegNet restores the image's spatial resolution using pooling index information, resulting in high-quality segmentation outcomes. Leveraged the advantages of SegNet, this study combined the strengths of U-Net and SegNet and incorporated the SE attention mechanism module to design a network structure, 2Se/U-Net, specifically for cervical cell image segmentation (Figure 1). The 2Se/U-Net network structure was similar to U-Net, retained the slice-based input processing approach, and included two main stages: encoding and decoding. The encoding stage consisted of four sets of convolutional blocks, with each block undergoing two convolution operations followed by ReLU activation functions. In the first three sets of convolutional blocks, a maximum pooling operation is performed after each convolution operation to progressively reduce the resolution of the feature maps.

The output from the fourth set of convolutional blocks is utilized as the input for the decoding stage. The decoding stage consists of three sets of convolutional blocks. After each set, a de-pooling operation is applied to progressively restore the resolution of the feature maps. Following upsampling, the outputs from each set of convolutional blocks on the left side are copied and concatenated with the corresponding inputs of the decoding stage's convolutional blocks to assist in detail recovery. Finally, the image restored to the original resolution undergoes convolution processing and outputs the final segmentation results through a Softmax layer.

The primary goal of the attention mechanism SE module's activation operation is to thoroughly understand the interdependencies between channels. This process involves two fully connected layers and two activation functions. First, the dimensionality and complexity are reduced using the first fully connected layer, followed by activation through the ReLU function. Next, the second fully connected layer restores the original depth and applies activation via the Sigmoid function. This process introduces additional nonlinear factors to model complex correlations between channels, integrates all input features, and maps the input parameters to a range between 0 and 1, thereby implementing a gating mechanism.

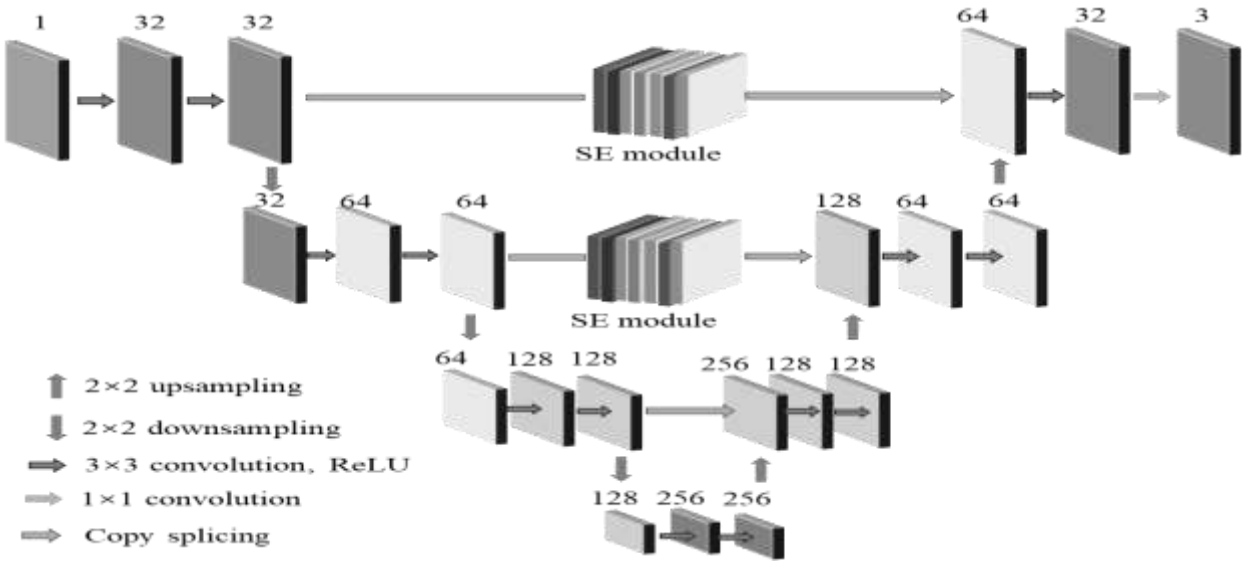

Figure 1: 2Se/U-Net network structure diagram.

The mathematical expression for the activation operation is given by Equation (1):

$A = \sigma[f(z, M)] = \sigma[M_2\delta(M_1 z)]$ (1)

In Equation (1), z represents the compressed global descriptor, δ denotes the ReLU function, and M1 and M2 are fully connected layers.

The attention mechanism SE module's reallocation operation aims to perform feature selection by adjusting the weights of the outputs after activation to determine the importance of each feature channel. Specifically, this involves multiplying these weight coefficients by the corresponding feature channels to achieve feature recalibration. This approach enhances the model's ability to discriminate between different channel features. The calculation method for the reallocation operation is expressed as Equation (2):

$Y = R_C * \mu_C$ (2)

In Equation (2), Rc represents the feature maps for each channel, and μc denotes the weight coefficients corresponding to these feature maps.

Conditional random fields (CRFs) were initially utilized for image denoising by smoothing noise to improve classification performance. CRFs enhance classification by coupling energy terms between adjacent nodes, making it more likely for nearby pixels to be classified into the same category, thus correcting errors in local filtering[13]. However, since the short-range connections of CRFs are primarily employed for smoothing the output image, they may overlook fine structures. To address potential over-smoothing and detail loss, this study employs fully connected CRFs (FC-CRFs). Its energy function is expressed as follows:

$E(x) = \sum_m \rho_m(x_m) + \sum_{mn} \rho_{mn}(x_m, x_n)$ (3)

$\rho_m(x_m) = -logP(x_m)$ (4)

In Equations (3) and (4), ρm(xm) represents the unary potential, x denotes the pixel label, and P(xm) refers to the pixel probability values output by the 2Se/U-Net network model.

The equation for calculating the binary potential of the 2Se/U-Net network model is expressed as Equation (5):

$\rho_{mn}(x_m, x_n) = \vartheta(x_m, x_n) \sum_{m=1}^{k} \alpha_m \cdot k^m (f_m, f_n)$ (5)

Where k^m is Gaussian kernel and α_m is the weight value.

Establishment of cervical cell image lesion recognition model based on ResNet

When processing cervical cell images, ResNet alleviates the vanishing gradient problem through residual connections, enabling the extraction of rich low-level features. However, its capability to capture subtle lesion features is limited. Lesions in cervical cell images often manifest as minute structural changes, which ResNet may not fully capture[14,15],

leading to suboptimal recognition performance. Additionally, the imbalance between the relatively few lesion samples and the abundant normal cell samples can cause ResNet to favor normal predictions, reducing the accuracy of lesion detection. To address these limitations, this study introduced a local discriminant loss function (LD-loss) and deep residual learning (DRL) residual blocks to optimize the model, establishing the LD/ResNet cervical cell image lesion detection model. The lesion detection process, which is illustrated in Figure 2, involved segmenting the collected cervical precancerous liquid-based cytology images using the 2Se/U-Net network model to obtain segmented images. These segmented images were then processed through the LD/ResNet network model for feature extraction, channel processing, and final classification by the discriminative module to produce the output results.

In the enhanced LD/ResNet network, a discriminative module and a novel channel attention mechanism are introduced. The purpose of the discriminative module is ensuring that feature channels possess effective discriminative regions for classification. The channel attention mechanism, on the other hand, maintains the discriminative power of each class's feature channels by randomly dropping a certain proportion of feature channels during training.[15]Consequently, the equation for the total loss function after optimization can be expressed as:

$$Loss(f) = L_{ce}(f) + \beta L_{ld}(f) \quad (6)$$

$$L_{ld}(f) = L_{di}(f) + \tau L_{di}(f) \quad (7)$$

Where β and τ are empirical values, with β set to 1.5 and τ set to 20. Lld represents the weighted sum of the discriminative component Ldi and the diversity component Ldi.

In the LD/ResNet network, each class is represented by a specific number of grouped feature channels. The discriminative module is utilized to impose constraints on these feature channels to ensure that each class's feature channels have sufficient discriminative power. The calculation equation for the discriminative module is expressed as:

$$L_{di}(f) = L_{ce}\left\{y, \frac{\left[e^{g(f_1)}, e^{g(f_2)}, \cdots, e^{g(f_{b-1})}\right]^t}{\sum_{m=0}^{c-1} e^{g(fm)}}\right\} \quad (8)$$

Evaluation of cervical cell image segmentation and precancerous lesion recognition performance

The segmentation performance of the model was evaluated using mean pixel accuracy (MPA) and mean intersection over union (mIoU). The calculation methods for MPA and mIoU are as follows:

$$\text{MPA} = \frac{1}{m+1}\sum_{i=0}^{m}\frac{P_{ii}}{\sum_{j=0}^{m}P_{ij}} \quad (9)$$

$$\text{mIoU} = \frac{1}{m+1}\sum_{i=0}^{m}\frac{P_{ii}}{\sum_{j=0}^{m}P_{ij}+\sum_{j=0}^{m}P_{ji}-P_{ii}} \quad (10)$$

In the equations, P_{ii} represents the number of true positives and true negatives; P_{ij} represents the number of false positives, and P_{ji} denotes the number of false negatives.

The model's ability to identify precancerous lesions was evaluated using Acc, Pre, recall (Re), and F1-score (F1). The calculation methods for these metrics are as follows:

$$\text{Acc} = \frac{T_p+T_N}{T_p+T_N+F_p+F_N} \quad (11)$$

$$\text{Pre} = \frac{T_p}{T_p+F_p} \quad (12)$$

$$\text{Re} = \frac{T_p}{T_p+F_N} \quad (13)$$

$$\text{F1} = 2 \times \frac{\text{Pre}\times\text{Re}}{\text{Pre}+\text{Re}} \quad (14)$$

In the equation, TP, TN, FP, and FN represent true positive, true negative, false positive, and false negative, respectively.

Test platform and test methods

All experiments were conducted on the same computational platform with the following configuration: CPU model Intel Xeon 8-core 2620V4, GPU model NVIDIA GTX 1080Ti, 64GB of memory (4 modules of 16GB each), Windows 10 operating system, TensorFlow 3.0 framework, and Python 3.6 programming language.

Cervical liquid-based cytology results were divided into training and testing groups in a 3:7 ratio. Based on the model's classification, cells were categorized into normal squamous epithelial cells (NS), normal intermediate squamous cells (NI), normal columnar cells (NC), mild squamous intraepithelial lesions (LD), moderate squamous intraepithelial lesions (MD), severe squamous intraepithelial lesions (SD), and carcinoma in situ (CIS).

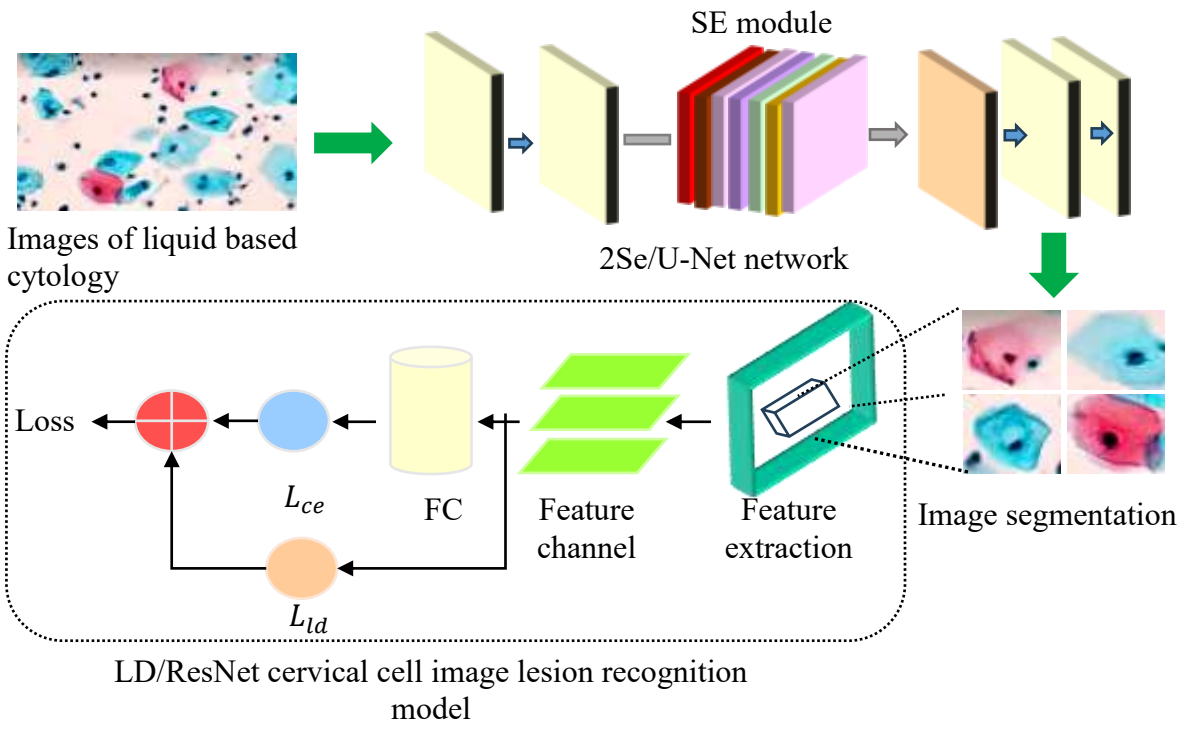

Figure 2: Identification of pathological changes in cervical cell images based on LD/ResNet

Statistical analysis

The experimental data were processed using *SPSS 19.0*. Quantitative data were expressed as mean ± standard deviation, while categorical data as percentages (%). The χ^2 test was adopted, and a *p*-value of <0.05 meant statistically significant.

Ethical considerations: The research protocol for this study had been approved by the Ethics Committee of Peking University First Hospital Ningxia Women and Children's Hospital. Prior to the commencement of the study, the ethics committee evaluated the scientific validity, necessity, and the potential risks and benefits of the research. During participant recruitment, strict adherence to the principle of voluntary participation was ensured. Participants voluntarily signed the informed consent form after being fully informed. Throughout the data collection and management process, personal information and medical data were strictly encrypted, and measures were taken to anonymize participants' identities in the research report and publication. Participants were free to withdraw from the study at any time for any reason.

Results

Comparison of segmentation indexes of cervical cell images before and after U-Net network optimization

In Figure 3, the U-Net model approaches convergence after the 13th complete training epoch, with both primary training metrics peaking during the 14th epoch, specifically achieving a MPA of 77.61% and a mIoU of 82.87%. In contrast, the 2Se/U-Net model begins to stabilize and converge after the 14th complete training epoch, reaching optimal performance by the 27th epoch, with the MPA increasing to 92.63% and the mIoU rising to 96.93%, representing improvements of 12.48% and 9.47% over the U-Net model, respectively.

Comparison of segmentation indexes of cervical cell images by different algorithms

The segmentation metrics of the 2Se/U-Net model are compared with those of the LFANet[16], AVM[17], U-Net[18], and GDLA[19] algorithms.

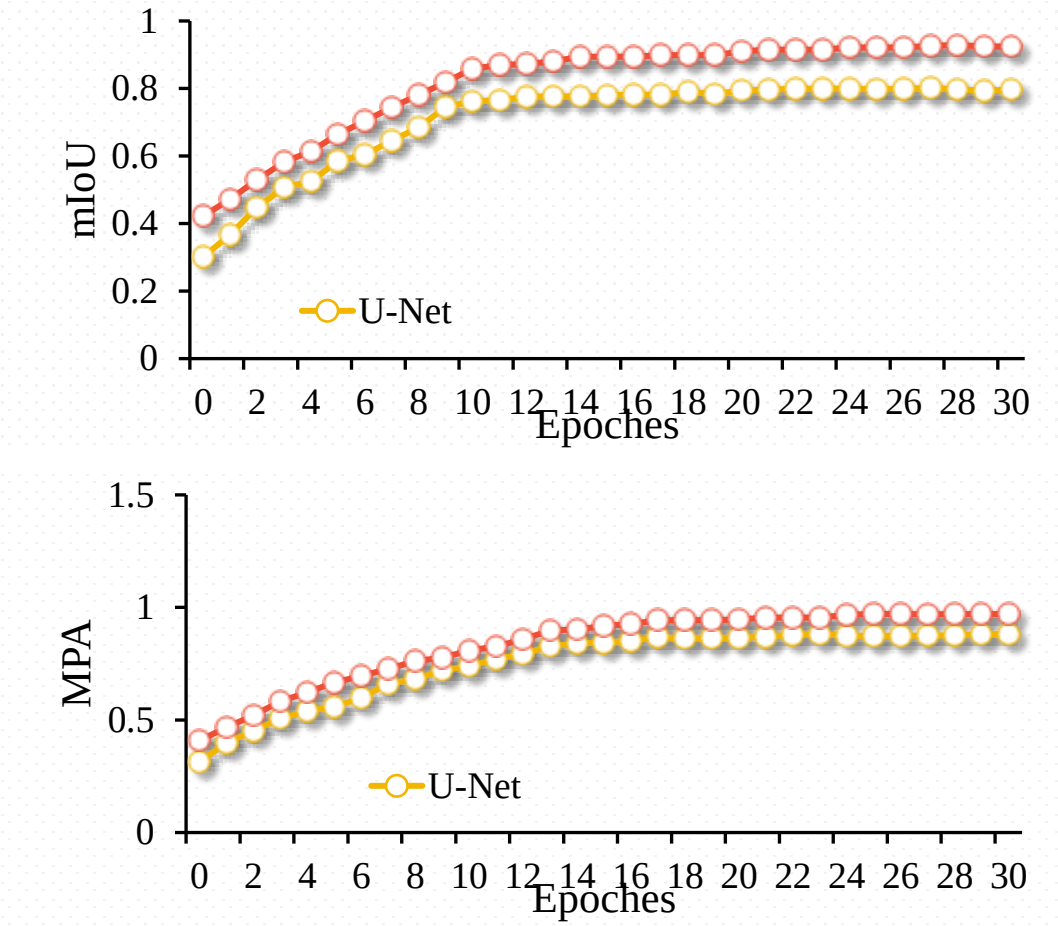

Figure 3: Comparison of segmentation indexes of cervical cell images under different iterations.

In Figure 4, the 2Se/U-Net model achieves a MPA of 97.32% and a mIoU of 97.02% for segmenting cervical cell images, which are markedly higher than those of the other four algorithms. Notably, the MPA and mIoU of the 2Se/U-Net model are drastically greater than the AVM and GDLA algorithms (p<0.05).

Comparison of cervical cell image lesion recognition performance before and after ResNet network optimization

The changes in loss values for cervical cell image lesion detection before and after optimization of the ResNet network are shown in Figure 5. As the number of iterations increases, the loss values for the ResNet, LD-loss, and LD/ResNet networks decrease, with the LD/ResNet network exhibiting the most pronounced reduction. At 100 iterations, the loss values for the ResNet, LD-loss, and LD/ResNet networks are 0.282, 0.150, and 0.050, respectively. Relative to ResNet and LD-loss, the loss value of the LD/ResNet network decreased by 0.228 and 0.096, respectively.

The variation in Acc for cervical cell image lesion detection before and after optimization of the ResNet network is depicted in Figure 6. As the number of iterations increases, the Acc of lesion detection improves for the ResNet, LD-loss, and LD/ResNet networks, with the LD/ResNet network showing the most significant increase. When the number of iterations reaches 100, the Acc values for the ResNet, LD-loss, and LD/ResNet networks are 94.43%, 95.54%, and 99.88%, respectively. Compared to ResNet and LD-loss, the Acc value of the LD/ResNet network has increased by 8.45% and 4.34%, respectively.

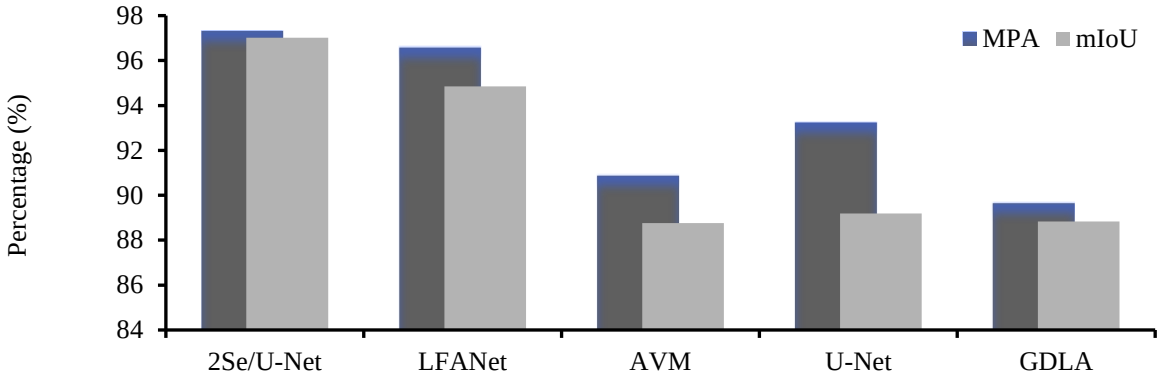

Figure 4: Comparison of segmentation indexes of cervical cell images by different algorithms.

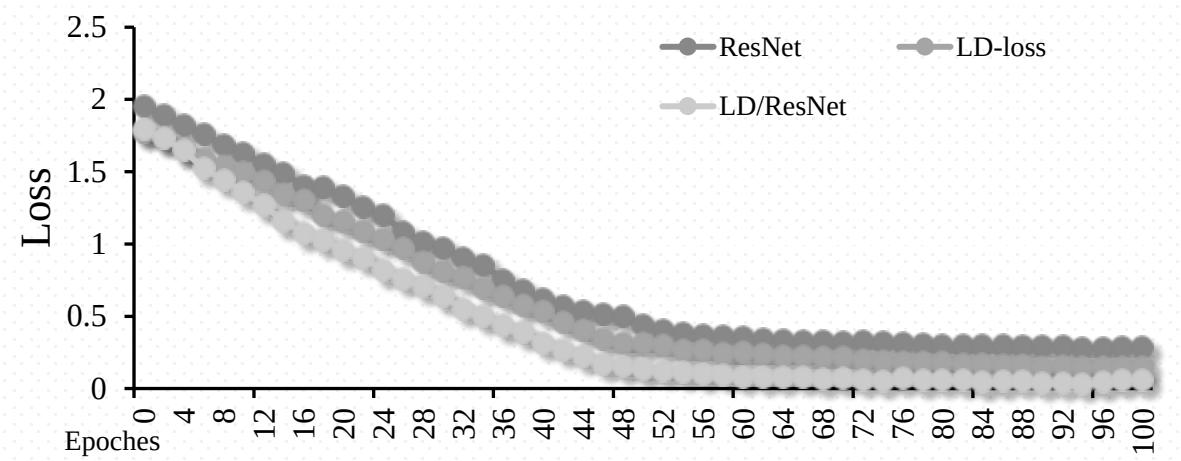

Figure 5: Comparison of Loss values of cervical cell image lesion recognition before and after ResNet optimization.

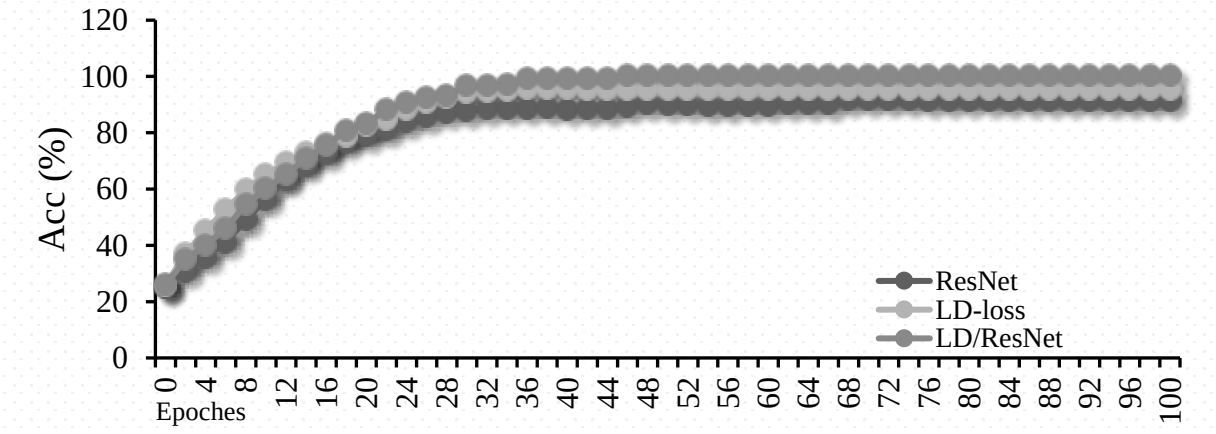

Figure 6: Comparison of Acc of cervical cell image lesion recognition before and after ResNet network optimization.

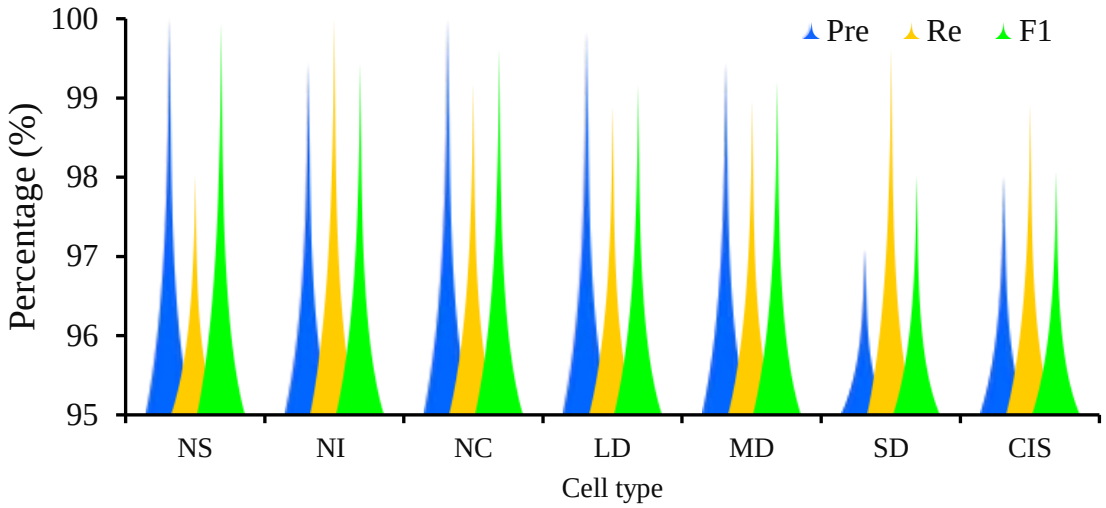

Figure 7: Comparison of identification indexes of different types of cervical cells in LD/ResNet network images

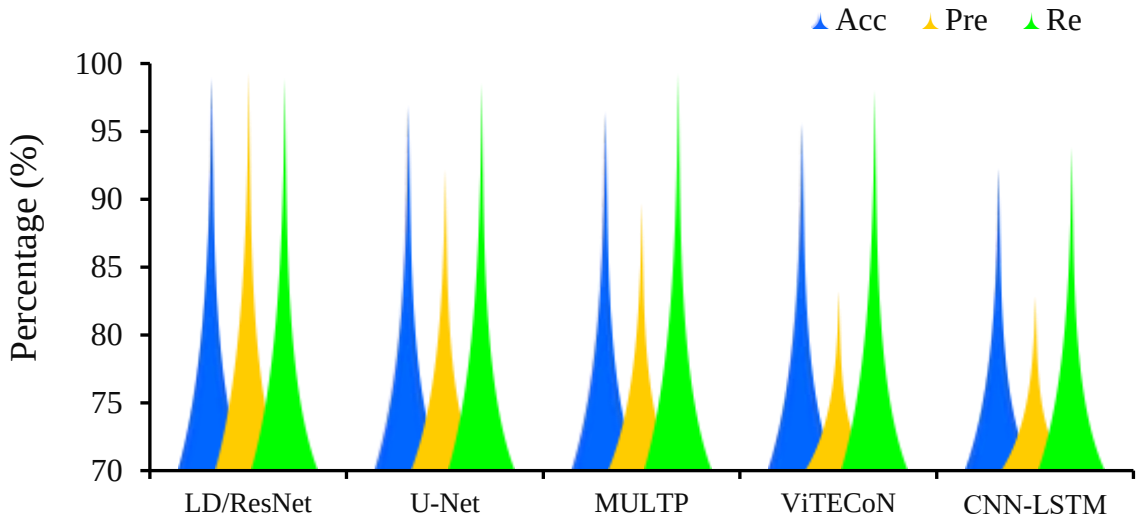

Figure 8: Comparison of identification indexes of precancerous lesions in cervical cell images with different algorithms.

Comparison of different types of cell identification indexes in LD/ResNet network cervical cell images

The statistical results for Acc, Re, and F1 score of the LD/ResNet network in identifying different types of cells in cervical cell images are presented in Figure 7. The LD/ResNet network achieves an Acc greater than 97.09%, with both Re and F1 scores exceeding 98.02% for distinguishing various cell types in cervical cell images.

Comparison of identification indexes of precancerous lesions in cervical cell images with different algorithms

The performance metrics of the LD/ResNet model for precancerous lesion detection in cervical cell

images are compared with those of the U-Net, MULTP[20], ViTECoN[21], and CNN-LSTM[22] algorithms. In Figure 8, the LD/ResNet model achieves an Acc of 98.95%, a Pre of 99.36%, and a Re of 98.89% in identifying precancerous lesions in cervical cell images, which are notably superior to those of the other four algorithms. Notably, relative to the CNN-LSTM algorithm, the LD/ResNet model demonstrated a drastic increase in Acc, Pre, and Re (p<0.05).

Discussion

The results indicate that the 2Se/U-Net model achieved improvements in MPA and mIoU by 12.48% and 9.47%, respectively, versus the U-Net model. These enhancements are attributed to the incorporation of an attention mechanism, which effectively improves the network's weight allocation to critical features[23]. The use of a de-pooling strategy during upsampling better preserves spatial pixel information, while the corresponding layer's concatenation operation optimizes multi-scale feature utilization[24], thus alleviating significant misidentification issues observed in previous experiments. The 2Se/U-Net model exhibited drastic increases in MPA and mIoU versus AVM and GDLA algorithms (p<0.05). This demonstrates that the 2Se/U-Net model excels in edge optimization for cell component segmentation, with both average pixel Acc and average intersection over union metrics exceeding 95%. This represents a notable improvement over the four other algorithms in cell component or nucleus segmentation under the same dataset, particularly highlighting the 2Se/U-Net's superior performance in edge detail segmentation for cervical cell images due to the irregular edge morphology and high-frequency information of the cell nuclei and cytoplasm.

Researchers[25-27] developed a cell segmentation model based on the U-Net architecture combined with data and image augmentation techniques. The model achieved a mIoU of 78% and a root mean square error close to 20%. Additionally, it demonstrated an Acc of 89%, with average Pre, Re, and F1 score of 89%, 89%, and 88.67%, respectively. This indicates that integrating CNN U-Net with image quality enhancement and data augmentation yields commendable results for segmenting cervical cell nuclei and cytoplasm. Researchers[28] established a cervical-UNet model for cervical cytology image segmentation, which achieved an object-level Acc of 93%, pixel-level Acc of 92.56%, object-level Re of 95.32%, pixel-level Re of 92.27%, a Dice coefficient of 93.12%, and an F1 score of 94.96%. The mIoU and segmentation Acc of the 2Se/U-Net model in our study surpass those of the aforementioned studies, indicating that the improvements in edge detail significantly enhance segmentation results. This outstanding performance in medical image segmentation holds substantial implications for advancing research and adoptions in the medical field.

The results show that the LD/ResNet model achieved accuracy, precision, and recall (Re)–of 98.95%, 99.36%, and 98.89%, respectively, in identifying precancerous lesions in cervical cell images, markedly outperforming the other four algorithms. Relative to the CNN-LSTM algorithm, the LD/ResNet model demonstrated a notable increase in Acc, Pre, and Re (p<0.05), indicating superior performance in precancerous lesion identification. In contrast, researchers[29] utilized an improved fuzzy C-means clustering algorithm, geometric and texture feature extraction, principal component analysis, and classification techniques for cervical cell image recognition, achieving a minimum Acc of 94.15%, a maximum Acc of 96.28%, an average Acc of 94.86%, sensitivity of 97.96%, specificity of 83.65%, an F1 score of 96.87%, and Pre of 96.31%. The LD/ResNet model in our study shows a prominent enhancement in image recognition Acc and Pre, suggesting that the optimized LD/ResNet model based on the ResNet network holds potential advantages in identifying precancerous lesions in cervical cell images.

Study strengths and limitations: The strength of this study lies in its innovative model, which combines U-Net and SegNet with the SE attention mechanism to construct the 2Se/U-Net segmentation model, and optimizes ResNet to develop the LD/ResNet lesion recognition model.

This significantly enhances the accuracy of cervical cell image segmentation and lesion detection, holding potential application value in assisting

clinicians with the early detection of precancerous lesions in the cervix of perimenopausal women. However, the study has a relatively small sample size of only 103 cases, lacks multi-center validation, and does not consider other factors such as hormone levels and medical history, which may impact the model's generalizability, accuracy, and reliability. Future studies will aim to expand the sample size, conduct multi-center validation, and integrate clinical information to further optimize the model.

Conclusion

This study aims to enhance the segmentation and identification of precancerous lesions in cervical cell images of perimenopausal women. By integrating the advantages of U-Net and SegNet and incorporating the attention mechanism SE module, an improved cervical cell image segmentation model, 2Se/U-Net, is developed. Simultaneously, an optimized LD/ResNet model for cervical cell image lesion identification is established by introducing LD-loss and DRL residual blocks into the ResNet network. Results demonstrate that the 2Se/U-Net model greatly improves segmentation outcomes versus the traditional U-Net model, showing superior performance. Additionally, the LD/ResNet model excels in identifying different types of cervical cells and precancerous lesions, significantly enhancing Acc and reliability. These improved segmentation and identification models based on U-Net and ResNet exhibit substantial adoption value in detecting precancerous lesions in perimenopausal women, effectively enhancing cervical cancer screening Acc and providing more reliable support for clinical diagnosis.

Funding

1.U-Net based deep learning colposcopy-assisted diagnosis of cervical lesions modeling Application and Research, (No.2023SF14)
2 Supported by the Natural Science Foundation of Ningxia, (No. 2023AAC03487), Supported by Ningxia Hui Autonomous Region Health and Wellness System Research Project, (No. 2023-NWKYT-006)

Authors contribution

Conceptualization, N.Z. and H.Y.M.; Methodology, N.Z. and H.Y.M.; Software, Y.C.; Validation, F.L. ,N.Z. and H.Y.M.; Formal Analysis, J.T.S. ; Investigation, Y.N.H. ; Resources, Y.C.; Data Curation, F.L. ; Writing – Original Draft Preparation, N.Z. and H.Y.M.; Writing – Review & Editing, N.Z. and H.Y.M.; Visualization, J.T.S. ; Supervision, Y.N.H.; Project Administration, N.Z. and H.Y.M.; Funding Acquisition, N.Z. and H.Y.M.

Conflicts of interest

The authors declare that they have no conflicts of interest.

References

1. Mansuri SM, Shrivastawa N and Parveen, N. Study on histopathological analycis at endometrium pattern in peri-menopause patient with abnormal uterine bleeding. *Journal of Cardiovascular Disease Research* 2024; 15: 06.
2. Liu X, Liu H, Xiong Y, Yang L, Wang C, Zhang R and Zhu X. Postmenopausal osteoporosis is associated with the regulation of SP, CGRP, VIP, and NPY. *Biomedicine & Pharmacotherapy* 2018; 104: 742-750.
3. AL-Qarawy AKM, AL-Obaidi ZME and Mohammad AK. Role of dehydroepiandrosterone hormone in relieving of vasomotor symptoms in post and peri menopause women. *In: Obstetrics and Gynaecology Forum.* 2024; 34(3): 105-108.
4. An H, Ding L, Ma M, Huang A, Gan Y, Sheng D and Zhang X. Deep Learning-Based Recognition of Cervical Squamous Interepithelial Lesions. *Diagnostics* 2023; 13(10): 1720.
5. Liu X, Yang R, Xiong T, Yang X, Li W, Song L and Geng L. CBCT-to-CT Synthesis for Cervical Cancer Adaptive Radiotherapy via U-Net-Based Model Hierarchically Trained with Hybrid Dataset. *Cancers* 2023; 15(22): 5479.
6. Shinohara T, Murakami K and Matsumura N. Diagnosis assistance in colposcopy by segmenting acetowhite epithelium using U-Net with images before and after acetic acid solution application. *Diagnostics* 2023; 13(9): 1596.
7. Huang Y, Zhu H, Wang P and Dong D. Segmentation of overlapping cervical smear cells based on U-Net and improved level set. *IEEE* 2019;3031-3035.
8. Wang J, Zhang B, Wang Y, Zhou C, Vonsky M S, Mitrofanova L B and Li Q. CrossU-Net: Dual-

modality cross-attention U-Net for segmentation of precancerous lesions in gastric cancer. *Computerized Medical Imaging and Graphics* 2024;112, 102339.
9. Desiani A, Utama Y, Arhami M, Affandi AK, Sasongko MA and Ramayanti I. Simple Data Augmentation and U-Net CNN for Neclui Binary Segmentation on Pap Smear Images. *Journal of Electronics, Electromedical Engineering, and Medical Informatics* 2024; 6(3): 264-275.
10. Teixeira JBA, Rezende MT, Diniz DN, Carneiro CM, Luz EJDS, Souza, MJ and Bianchi AGC. Segmentation of cervical nuclei using convolutional neural network for conventional cytology. *Computer Methods in Biomechanics and Biomedical Engineering: Imaging & Visualization* 2023; 11(5): 1876-1888.
11. Liu H and Tang T. MAPK signaling pathway-based glioma subtypes, machine-learning risk model, and key hub proteins identification. *Scientific Reports* 2023; 13(1): 19055.
12. Zhang C, Lu W, Wu J, Ni C and Wang H. SegNet Network Architecture for Deep Learning Image Segmentation and Its Integrated Applications and Prospects. *Academic Journal of Science and Technology* 2024; 9(2): 224-229.
13. Zhou S, Li X, Fu Y, Ouyang X, Yang J, Grzegorzek M and Li C. High Order Conditional Random Field Based Cervical Cancer Histopathological Image Classification. In: International Conference on Image, Vision and Intelligent Systems. Singapore: Springer Nature Singapore 2023; 3-16.
14. Fauzi H, Ansori RB, Siadari T, Harsono AB and Rahmah QN. Classification of Cervical Cancer Images Using Deep Residual Network Architecture. *International Journal of Artificial Intelligence Research* 2023; 7(1): 56-63.
15. Liu Y, Chen C, Xie X, Lv X and Chen C. For cervical cancer diagnosis: Tissue Raman spectroscopy and multi-level feature fusion with SENet attention mechanism. *Spectrochimica Acta Part A: Molecular and Biomolecular Spectroscopy* 2023; 303: 123147.
16. Zhao Y, Fu C, Xu S, Cao L and Ma HF. LFANet: Lightweight feature attention network for abnormal cell segmentation in cervical cytology images. *Computers in Biology and Medicine* 2022; 145: 105500.
17. Alquran H, Mustafa WA, Qasmieh IA, Yacob YM, Alsalatie M, Al-Issa Y and Alqudah AM. Cervical cancer classification using combined machine learning and deep learning approach. *Comput Mater Contin* 2022; 72(3): 5117-5134.
18. Nazir N, Sarwar A, Saini BS and Shams R. A robust deep learning approach for accurate segmentation of cytoplasm and nucleus in noisy pap smear images. *Computation* 2023; 11(10): 195.
19. Li G, Sun C, Xu C, Zheng Y and Wang K. Cervical cell segmentation method based on global dependency and local attention. *Applied Sciences* 2022; 12(15): 7742.
20. Fekri-Ershad S and Ramakrishnan, S. Cervical cancer diagnosis based on modified uniform local ternary patterns and feed forward multilayer network optimized by genetic algorithm. *Computers in Biology and Medicine* 2022; 144: 105392.
21. Shiny TL and Parasuraman K. ROI Extraction and Nuclei Classification of Pap Smear Images for Cervical Cancer Detection. In: 2023 2nd International Conference on Vision Towards Emerging Trends in Communication and Networking Technologies (ViTECoN). *IEEE* 2023; 1-7.
22. Chitra B and Kumar SS. Early cervical cancer diagnosis using Sooty tern-optimized CNN-LSTM classifier. *International Journal of Imaging Systems and Technology* 2022; 32(6): 1846-1860.
23. Li G, Shi G and Jiao J. YOLOv5-KCB: A new method for individual pig detection using optimized K-means, CA attention mechanism and a bi-directional feature pyramid network. *Sensors* 2023; 23(11): 5242.
24. Zhang Q, Liang Y, Zhang Y, Tao Z, Li R and Bi H. A comparative study of attention mechanism based deep learning methods for bladder tumor segmentation. *International Journal of Medical Informatics* 2023; 171: 104984.
25. Rose MM, Dhamodharan S, Revathidevi S, Chakkarappan SR, Jagadeesan MG, Subbiah S and Munirajan, AK. High incidence of PI3K pathway gene mutations in South Indian cervical cancers. Cancer Genet. 2022; 264-265: 100-108.
26. Özbay E and Özbay FA. Interpretable pap-smear image retrieval for cervical cancer detection with rotation invariance mask generation deep hashing. *Computers in Biology and Medicine* 2023; 154: 106574.
27. Rudiansyah R, Iryani, L, Kesuma LI, Sari P and Alamsyah A. Combination of Image Enhancement and U-Net Architecture for Cervical Cell Semantic Segmentation. *JOURNAL OF INFORMATICS AND TELECOMMUNICATION ENGINEERING* 2024; 7(2): 575-586.
28. Rasheed A, Shirazi SH, Umar AI, Shahzad M, Yousaf W and Khan Z. Cervical cell's nucleus segmentation through an improved UNet architecture. *Plos one* 2023; 18(10): e0283568.
29. Lavanya Devi N and Thirumurugan P. Cervical cancer classification from pap smear images using modified fuzzy C means, PCA, and KNN. *IETE Journal of Research* 2022; 68(3): 1591-1598.